Available online at www.sciencedirect.com
SCIENCE DIRECT
Developmental Biology 291 (2006) 239–252
DEVELOPMENTAL BIOLOGY
www.elsevier.com/locate/ydbio

ARI-1, an RBR family ubiquitin-ligase, functions with UBC-18 to regulate pharyngeal development in *C. elegans*

Xiaohui Qiu, David S. Fay *

Department of Molecular Biology, University of Wyoming, P.O. Box 3944, Laramie, WY 82071-3944, USA

Received for publication 24 June 2005; revised 25 October 2005; accepted 29 November 2005
Available online 7 February 2006

Abstract

The LIN-35 retinoblastoma protein homolog and the ubiquitin-conjugating enzyme UBC-18 function redundantly to control an early step of pharyngeal morphogenesis in *C. elegans*. In order to identify ubiquitin-ligases acting downstream of UBC-18, we carried out a two-hybrid screen using UBC-18 as the bait molecule. Our screen identified three putative ubiquitin-ligases, one of which, ARI-1, showed genetic interactions leading to defective pharyngeal development that were identical to that previously observed for UBC-18. ARI-1 is a member of the RBR family of ubiquitin-ligases and contains a C-terminal motif that places it within the highly conserved Ariadne subfamily of RBR ligases. Our analyses indicate that ARI-1 is the principal Ariadne family member in *C. elegans* that is involved in the control of pharyngeal development with UBC-18. Using GFP reporters, we find that ARI-1 is expressed dynamically in a wide range of tissues including muscles and neurons during embryonic and postembryonic development. We also provide evidence that dsRNA species containing 14 or fewer base pairs of contiguous identity with closely related mRNAs are sufficient to mediate off-target silencing in *C. elegans*.

Keywords: *lin-35*; Retinoblastoma; *ubc-18*; *ari-1* ubiquitin; *C. elegans*; Pharynx; Ariadne

Introduction

The regulation of protein stability through ubiquitin-mediated proteolysis has been shown to play a critical role in a wide range of cellular and developmental processes. For example, in *C. elegans*, the ubiquitin pathway controls cell polarity and asymmetric cell division in the early embryo, a process that is essential for the precise segregation of maternal determinants and establishment of the anterior–posterior axis (Cowan and Hyman, 2004; Levitan et al., 1994; Rappleye et al., 2002). Correspondingly in mammals, the ubiquitin-ligase Smurf1 targets degradation of the small GTPase RhoA, thereby controlling cytoskeletal dynamics and consequent changes in cell polarity and shape, and in epithelial cell differentiation (Bryan et al., 2005; Ozdamar et al., 2005; Wang et al., 2003). Other roles for ubiquitin and ubiquitin-like molecules have been described in *C. elegans* including the regulation of cell cycle progression (Fay et al., 2002; Feng et al., 1999; Kipreos et al., 1996, 2000; Kitagawa et al., 2002; Kurz et al., 2002; Shakes et al., 2003; Zhong et al., 2003), germline establishment and meiosis (DeRenzo et al., 2003; Furuta et al., 2000; Golden et al., 2000; Pintard et al., 2003; Yeong, 2004), cell signaling (Hubbard et al., 1997; Liao et al., 2004; Yoon et al., 1995), and morphogenesis (Fay et al., 2003; Nayak et al., 2002), in addition to other functions.

The process by which cellular proteins become marked for destruction is mediated by a series of hierarchical enzymes (termed E1 to E4) that lead to the covalent attachment of a ubiquitin moiety to the target substrate (Glickman and Ciechanover, 2002; Pickart, 2001). Initially, a broad-spectrum ubiquitin-activating enzyme (E1) transfers the 76-amino-acid ubiquitin peptide via a thiol ester intermediate to a ubiquitin-conjugating enzyme (E2/UBC). The E2 then associates with a ubiquitin-ligase enzyme (E3), which is required for the transfer of ubiquitin to a specific lysine residue within the target protein. The E3 enzymes are generally credited with providing specificity to the process. Additional ubiquitin monomers may then be consecutively added by a distinct ubiquitin-ligase enzyme (E4) to produce the poly-ubiquitinated product that

* Corresponding author. Fax: +1 307 766 5098.
E-mail address: davidfay@uwyo.edu (D.S. Fay).

0012-1606/$ - see front matter © 2005 Elsevier Inc. All rights reserved.
doi:10.1016/j.ydbio.2005.11.045

serves as a substrate for degradation by the 26S proteasome (Hatakeyama and Nakayama, 2003). Alternatively, substrates marked with one or several ubiquitins may be targeted for endocytosis and transport to lysosomes, or may remain in the cell, albeit with altered activities (Hicke, 2001; Schnell and Hicke, 2003).

In most organisms, there is a single E1, a sizeable but limited number of E2s, and a large number of E3s. For example, in *C. elegans*, there is one E1, ~23 E2s, and >130 putative E3s, the majority of which contain either a RING or HECT domain. A general model to have emerged is that most E2s probably act in conjunction with multiple E3s, and that individual E3s are themselves likely to recognize multiple target substrates (Castro et al., 2005; Glickman and Ciechanover, 2002; Pickart, 2001). Further adding to the complexity of the system is the existence of E3s that are composed of multiple subunits such as the Skp1–cullin–F-box-protein complex (SCF) and the anaphase-promoting complex/cyclosome (APC; Castro et al., 2005; Petroski and Deshaies, 2005). In particular, given the large number of Skp1 and F-box proteins encoded by most genomes (the *C. elegans* genome encodes 21 Skp-1-related proteins and >300 F-box proteins), there exists the potential for an impressively large number of subunit combinations, each of which may have distinct functions and enzymatic properties (Kipreos and Pagano, 2000; Nayak et al., 2002).

The RING finger class of E3 ligases encompasses a large number of distinct family members, some of which function within large multisubunit complexes and many others that act as single subunits or homodimers (Glickman and Ciechanover, 2002; Pickart, 2001). One such family member, the RBRs (for RING-Between rings-RING), includes most notably the human disease gene Parkin; mutations in Parkin are the leading cause of hereditary parkinsonism, although the underlying etiological mechanism is not well understood (Kahle and Haass, 2004; Kitada et al., 1998; Marin et al., 2004). RBR family ligases contain two C_3HC_4 RING fingers that are separated by a unique C_6HC domain that has been called the IBR (in-between-RINGS) or DRIL (double RING finger-linked) domain (Morett and Bork, 1999; van der Reijden et al., 1999). The precise function of the IBR/DRIL domain, as well as the C-terminal RING finger of RBR ligases, is currently unclear (Aguilera et al., 2000; Ardley et al., 2001; Moynihan et al., 1999). RBR ligases are generally thought to function as single-subunit E3s, although a noteworthy gene fusion between one family member and a cullin gene has led to the suggestion that RBRs may in some cases function within larger complexes (Marin and Ferrus, 2002; Marin et al., 2004). RBR family members include the Parkin, Dorfin, Plant I/II, ARA54, XAP3, and Ariadne subfamilies; the last group seems to be the most ancient and predates the origin of plants, animals, and fungi (Marin and Ferrus, 2002).

We have previously shown that the ubiquitin-conjugating enzyme UBC-18 functions in a parallel pathway to LIN-35, the *C. elegans* Retinoblastoma/pocket protein homolog, to regulate an early step in pharyngeal morphogenesis (Fay et al., 2003). Whereas single mutants in *ubc-18* and *lin-35* show no obvious defects, *lin-35; ubc-18* double mutants are nonviable because (at least in part) of the inability to consume nutrients. The defect in pharyngeal development affects the ability of the anterior-most pharyngeal cell precursors to undergo a stereotypical reorientation in their apical-basal polarities (Fay et al., 2003; Portereiko and Mango, 2001). This in turn leads to the failure of the primordial pharynx to attach to the mouth (or buccal cavity), resulting in a misshapen nonfunctional organ. We have also demonstrated a role for a third protein, PHA-1, in the processes of pharyngeal morphogenesis (Fay et al., 2004). Based on genetic evidence, PHA-1 appears to constitute an additional redundant pathway with LIN-35 and UBC-18. Whereas a partial reduction in *pha-1* activity has little or no effect on viability, double mutants with *pha-1* and either *lin-35* or *ubc-18* are lethal and display the identical phenotype to *lin-35; ubc-18* double mutants.

We report here the identification of the downstream E3 partner of UBC-18 in pharyngeal development, ARI-1. ARI-1 is a member of the highly conserved Ariadne subfamily of RBR ligases. Interestingly, the phenotypes and expression patterns of the *ariadne* orthologs in worms and flies suggest that Ariadne family functions may be partially conserved across species (Aguilera et al., 2000).

Materials and methods

Strains

Maintenance, culturing, and genetic manipulation of *C. elegans* were carried out following standard procedures at 16°C and 20°C (Steirnagle, 2005; www.wormbook.org). Strains used in the phenotypic analysis include N2, DP38 [*unc-119(ed3)*], PD4792 [mIs11 IV *myo-2*: :GFP], MH1384 [kuIs46 X *ajm-1*: :GFP], WY83 [*lin-35; ubc-18; kuEx119*], WY162 [*pha-1(e2123)*; *sup36*], WY164 [*pha-1(e2123)*; *sup37*], WY180 [*pha-1(e2123)*; *myo-2*: :GFP], WY131 [*vab-7 (e1562), pha-1(e2123)*; *ajm-1*: :GFP], NL2099 [*rrf-3(pk1426)*], and GE24 [*pha-1(e2123)*]. The extrachromosomal array *kuEx119* expresses both wild-type *lin-35* as well as a ubiquitously expressed GFP reporter (*sur-5*: :GFP; Fay et al., 2002).

Two-hybrid screen and assays

PCR amplification for bait and prey constructs was carried out using Pfu DNA polymerase (Stratagene), and all resulting constructs were confirmed by sequence analysis. The bait construct containing the full-length UBC-18 cDNA was fused in frame to the GAL4 DNA-binding domain (DB) using Gateway cloning methods (pDEST32; Invitrogen) and suitable primers 5′-ggggacaagtttg-tacaaaaaagcaggcttgatgtcagcgacacg-3′/5′-ggggaccactttgtacaagaaagctgggtactatt-caggccgctt-3′. The bait construct was introduced into yeast strain Mav203 and failed to activate the three reporter genes (*HIS3*, *URA3*, and *lacZ*) together with the empty prey vector pEXP-AD502. Sequential transformation was carried out to introduce the cDNA prey library (ProQuest pre-made cDNA library, Invitrogen). From ~5×10^5 yeast colonies, 110 were identified that grew on the synthetic medium lacking Leu, Trp, and His and containing 75 mM 3-amino-1,2,4-triazole (3AT). Thirty-three of the 110 isolates were also positive for two other reporter genes, *URA3* and *lacZ*. The prey plasmids were rescued from positive yeast strains into *E. coli*. They were then retransformed into Mav203 together with the DB–UBC-18 construct or the empty bait vector (pDBLeu) and examined for induction of the reporter genes. Positive prey vectors that induced all three reporter genes in the presence of the DB–UBC-18 construct but not in the presence of pDBLeu (no-insert control), were sequenced to identify the inserts.

For the DB–ARI-1 construct, full-length *ari-1* cDNA was released from the prey construct by *Not*I and *Sac*I and subcloned in vector pDBLeu in frame with the GAL4 DNA-binding domain. N-terminally truncated *ari-1* was amplified using suitable primers: *ari-1*Δ19 (lacking the first 19 N-terminal amino acids),

5′-ggggacaagtttgtacaaaaaagcaggcttggacgatgggtgtat-3′/5′-ggggaccactttgtacaagaaagctgggtattactcgttgaaaac-3′; *ari-1*Δ42 (lacking the first 42 N-terminal amino acids), 5′-ggggacaagtttgtacaaaaaagcaggcttgaaagataacgggga-3′/5′-ggggaccatttgtacaagaaagctgggtattactcgttgaaaac-3′; *ari-1*Δ123 (lacking the first 123 N-terminal amino acids), 5′-ggggacaagtttgtacaaaaaagcaggcttgggagacgcggaatg-3′/5′-ggggaccactttgtacaagaaagctgggtattactcgttgaaaac-3′; *ari-1*Δ178 (lacking the first 178 N-terminal amino acids), 5′-ggggacaagtttgtacaaaaaagcaggcttggaagatgaaaaggt-3′/5′-ggggaccactttgtacaagaaagctgggtattactcgttgaaaac-3′; *ari-1*$_{43–191}$ (containing the region from amino acid 43 to 191), 5′-ggggacaagtttgtacaaaaaagcaggcttgaaagataacgggga-3′/5′-ggggaccac tttgtacaagaaagctgggtattatgttgggtcggt-3′. For the activation domain (AD)–*ubc-18* construct, full-length *ubc-18* was amplified using the following primers: 5′-ggggacaagtttgtacaaaaaagcaggcttgatgtcagcgacacg-3′/5′-ggggaccactttgtacaagaaagctgggtactattcaggccgctt-3′. Using Gateway methods, fragments were subcloned using pDEST32 and PDEST22 to make the *ari-1* bait and *ari-1* and *ubc-18* prey constructs, respectively.

For the construction of AD–C27A12.6 and AD–C27A12.7 vectors, full-length C27A12.6 and C27A12.7a were PCR amplified using suitable primers: C27A12.6, 5′-ggggacaagtttgtacaaaaaagcaggcttgatgaattcagacga-3′/5′-ggggaccactttgtacaagaaagctgggtattatcaatcgttgta-3′; C27A12.7a, 5′-ggggacaagtttgtacaaaaaagcaggcttgatgaattctgacgc-3′/5′-ggggaccactttgtacaagaaagctgggtattatcactcgttgta-3′. Fragments were then subcloned into pDEST22 using Gateway methods.

GST pull-down assays

A full-length cDNA of UBC-18 was cloned into the *Bam*HI and *Eco*RI sites of pGEX-2T (Amersham Biosciences) to create an in frame fusion with Glutathione *S*-transferase (GST). Two primers (5′-ggatcctaatacgactcactataggagccaccatgagttccgac-3′/5′-taattactcgttgaaaaccca-3′) were used to amplify an *ari-1* full-length cDNA containing an upstream bacteriophage T7 promoter and a kozak sequence using Pfu DNA polymerase. This PCR product was sequenced and used to generate ^{35}S-methionine radiolabeled ARI-1 in vitro using the TNT T7 Quick for PCR DNA system (Promega). To perform the binding assay, GST–UBC-18 or GST alone was purified from a 12 ml culture using BugBuster Master Mix (Novagen) 2.5 h after induction by 0.5 mM IPTG, and were incubated with 16 μl of ^{35}S-radiolabeled ARI-1 in 200 μl of 1× PBS binding buffer (0.14 M NaCl, 2.7 mM KCl, 10.1 mM Na_2HPO_4, and 1.8 mM KH_2PO_4, pH7.3) in the presence of protease inhibitor Leupeptin (0.5 μg/ml) at room temperature for half an hour. After washing the beads five times with 1× PBS (500 μl per wash) and releasing the proteins from the column with glutathione elution buffer, bound proteins were analyzed by SDS-PAGE (10% acylamide gel) and detected by Coomassie staining and autoradiography.

RNAi

RNAi feeding and injection were carried out following standard methods (Fire et al., 1998; Fraser et al., 2000; Timmons et al., 2001). The constructs for Y65B4BR.4; F56D2.2; T12E12.1; and the "central" coding regions of C27A12.6, C27A12.7, and *ari-1* were obtained from the MRC RNAi library (Fraser et al., 2000; Kamath et al., 2003). The "central coding region" constructs for *ari-1* paralogs correspond to the following: C27A12.6, 17,993–19,175 of cosmid C27A12, 70–1183 of the 1476 bp spliced coding region, and spanning exons 2–5 of the six-exon gene; C27A12.7, 20,662–21,850 of cosmid C27A12, 1–882 of the 1476 bp spliced coding region, and spanning exons 2–5 of the eight-exon gene; *ari-1*, 22,920–24,119 of cosmid C27A12, 185–1105 of the 1485 bp spliced coding region, and spanning exons 2–5 of the seven-exon gene. All other constructs for RNAi feeding were made by cloning appropriate genomic fragments into the polylinker of PD129.36 and the recombinant vectors were transformed into HT115(DE3) *E. coli*. For Y73F8A.34, the fragment used for RNAi feeding corresponds to nucleotides 300,943–301,344 of Y73F8A.34. 3′ UTR RNAi-feeding constructs for C27A12.6, C27A12.7, and *ari-1* correspond to sequences 17,281–17,457, 19,442–19,751, and 22,045–22,206 of C27A12, respectively. The "5′ coding region" RNAi-feeding constructs of the *ari-1* paralogs correspond to the following: C27A12.6, 18,983–19,300 of cosmid C27A12, 1–216 of the 1476 bp spliced coding region, and spanning exons 1–3 of the six-exon gene; C27A12.7, 21,388–21,709 of cosmid C27A12, 1–230 of the 1476 bp spliced coding region, and spanning exons 1–3 of the eight-exon gene; *ari-1*, 23,959–24,432 of cosmid C27A12, 1–220 of the 1485 bp spliced coding region, and spanning exons 1–3 of the seven-exon gene.

Double-stranded RNA for injection was made from templates generated by PCR from each of the following primer sets to which T7 polymerase promoter sites had been added: C27A12.6, 5′-tgcttgaccacgattcat-3′/5′-tcatgccagttttgtcca-3′; C27A12.7, 5′-tgaacacgacgatagctg-3′/5′-gccacaagagaaacagaa-3′; *ari-1*, 5′-tctgacgatgatggcatc-3′/5′-tgagcaatttgcaatttg-3′; Y73F8A.34, 5′-tgctctggaatccgacat-3′/5′-tcctcgataagcaacttg-3′; T12E12.1, 5′-aagactactacaacgaag-3′/5′-caacatgactcttccaac-3′. Following sequencing confirmation of the PCR products, dsRNA (1.0–1.5 mg/ml) was injected into the syncitial gonad arms of N2 and *rrf-3* mutants, and progeny were examined for effects.

ARI-1::*GFP expression*

A genomic region spanning nucleotide positions 21,709 to 25,416 of cosmid C27A12 was cloned into the *Spe*I and *Xho*I sites of pBluescript KS+ (using primers 5′-aagactagtcgacagtttttggcgagaaattc-3′/5′-gtagactcgagtgctgaataggaaaaatgaggaga-3′) to generate plasmid pDF76, which was sequenced and found to contain no alterations from the published sequence. The region includes the entire *ari-1* coding region as well as 984-bp of upstream and 627-bp of downstream regulatory sequences, which encroach into the neighboring genes C27A12.9 and C27A12.7, respectively. *Hind*III and *Bam*HI sites were introduced into the N- and C-terminal coding region of *ari-1*, respectively, using the QuikChange XL kit from Stratagene. The *Hind*III site was inserted directly downstream from the start ATG to generate the new sequence 5′-ATGAAGCTTAGT-3′ (pDF79). The *Bam*HI site was inserted 18-bp upstream from the stop codon of *ari-1* to generate the new sequence 5′-GATGGATCC-CAA-3′ (pDF82). GFP(S65C) was amplified from plasmid pPD95.77 (gift of A. Fire) and inserted into the *Hind*III site of pDF79 and the *Bam*HI site of pDF82 to generate pDF90 and pDF87, respectively. Both plasmids were sequenced to verify preservation of the reading frame as well as the absence of any mutations in the GFP coding region. Rescuing sequences for *unc-119* were further inserted into the *Not*I and *Sac*II sites of pDF90 and pDF87, to generate plasmids pDF92 and PDF91, respectively. Extrachromosomal lines were generated by microinjection of pDF87 and pDF90 using *rol-6* (pRF4) and by microbombardment using the biolistic PDS-1000/He unit from BioRad with plasmids pDF91 and pDF92 and strain DP38 [*unc-119(ed3)*] (Mello et al., 1991; Praitis et al., 2001). Bombardment was also used to generate low-copy integrated lines for plasmids pDF91 and pDF92, although these lines failed to express GFP at appreciable levels. Integration of the extrachromosomal array containing plasmid pDF92 (WY223; *fdEx9*) was achieved by gamma-irradiation to generate strain WY246 (*fdIs9*). WY222 is a strain carrying an extrachromosomal array (*fdEx10*) of plasmid pDF91 generated by bombardment.

In situ hybridization

In situ hybridization was carried out according to established protocols (Mochii et al., 1999) using commercially available reagents for DIG labeling and visualization (Roche). The sense (control) and antisense (experimental) probes span nucleotides 73–896 and 67–532 of the *ari-1* mRNA, respectively.

Results

A two-hybrid screen with UBC-18 identified three ubiquitin-ligases

We had previously identified the putative ubiquitin-conjugating enzyme *ubc-18* as a co-regulator of pharyngeal development with *lin-35*/Rb and *pha-1* (Fay et al., 2003, 2004). To identify potential E3 ligases that function as partners of UBC-18, we carried out a yeast two-hybrid screen using a full-length UBC-18 fusion to the GAL4–DNA binding domain (DB–UBC-18) as the bait molecule (for details, see Materials and methods). From a screen of ~5×10^5 colonies, 33 positive clones were identified that resulted in the strong activation of three independent reporter constructs (*HIS3*, *URA3*, and *lacZ*) in

yeast (Table 1 and Fig. 1). Activation of the reporter genes was dependent on the presence of the DB–UBC-18 bait construct, indicating that reporter activation did not result from nonspecific activation by the GAL4-activation domain (AD; prey) fusion isolates (Table 1). As determined by sequence analysis and PCR screening, the positive clones represented three separate genes: Y65B4BR.4/*wwp-1* (for *WW* domain protein), 28 clones; F56D2.2, 2 clones; and C27A12.8/ARI-1, 3 clones (Fig. 1 and Table 1). Notably, WWP-1 contains a HECT domain, whereas both F56D2.2 and ARI-1 contain the Zn-finger variants known as RING fingers. Given that both HECT and RING-finger domains are found in many ubiquitin-ligases, it seems probable that all three proteins function as co-partners of UBC-18 in vivo.

For reasons described below, we further tested for the ability of ARI-1 in the bait configuration to interact with UBC-18 in the prey configuration. In carrying out these experiments, we found that the full-length DB–ARI-1 fusion resulted in a substantial level of reporter activation in the presence of the empty-vector prey construct (Table 1). Based on several of the ARI-1 clones isolated by our initial screen, it appeared that the N terminus of ARI-1 was not essential for its interaction with UBC-18 (data not shown). We therefore constructed several deletion variants of ARI-1 and found that removal of either 19 or 42 amino acids from the N terminus of ARI-1 abrogated autoactivation of the reporters by the bait construct. Importantly, both deletion variants showed clear interactions with a full-length AD–UBC-18 fusion, further evidence of a physical interaction (Table 1). However, we note that the strength of the observed interaction between ARI-1(Δ42) and UBC-18, as judged by the *lacZ* assay, was reduced compared to that of full-length ARI-1 (data not shown).

To further verify the physical interaction between *C. elegans* ARI-1 and UBC-18, we expressed a fusion of full-length UBC-18 to GST in *E. coli* and tested for its ability to bind ^{35}S-labeled full-length ARI-1. As shown in Fig. 2, ^{35}S-ARI-1 bound specifically to GST–UBC-18, but not to GST alone, providing additional support for this interaction.

Table 1
Two-hybrid interactions

Vectors	*LEU2/TRP1*	*HIS3*[a]	*URA3*[a]	*lacZ*
DB–UBC-18/pEXP-AD502	+	−	−	−
DB–UBC-18/AD–Y65B4BR.4	+	+	+	+
DB–UBC-18/AD–F56F2.2	+	+	+	+
DB–UBC-18/AD–ARI-1	+	+	+	+
pDBLeu/AD–Y65B4BR.4	+	−	−	−
pDBLeu/AD–F56F2.2	+	−	−	−
pDBLeu/AD–ARI-1	+	−	−	−
DB–UBC-18/AD–C27A12.6	+	+	−	−
DB–UBC-18/AD–C27A12.7	+	−	−	−
DB–ARI-1/pEXP-AD502	+	+	+	+
DB–ARI-1(Δ19)/pEXP-AD502	+	−	−	−
DB–ARI-1(Δ42)/pEXP-AD502	+	−	−	−
DB–ARI-1(Δ19)/AD–UBC-18	+	+	+	+
DB–ARI-1(Δ42)/AD–UBC-18	+	+	+	+
DB–UBC-18/AD–ARI-1(Δ42)	+	+	+	+
DB–UBC-18/AD–ARI-1(Δ123)	+	−	−	−
DB–UBC-18/AD–ARI-1(Δ178)	+	−	−	−
DB–UBC-18/AD–ARI-1(43–191)	+	−	−	−
DB–ARI-1(Δ19)/AD–ARI-1	+	−	−	−
DB–ARI-1(Δ19)/AD–C27A12.6	+	−	−	−
DB–ARI-1(Δ19)/AD–C27A12.7	+	−	−	−

For details on constructs and experimental procedures, see Materials and methods.

+/− indicates growth ability on SD-minus plates lacking leucine (Leu), tryptophan (Trp), histodine (His), and uracil (Ura) as well as the ability to activate expression of a β-galactosidase reporter. DB vectors contain the GAL4 DNA-binding domain (bait construct), whereas AD vectors contain the GAL4 transactivation domain (prey construct). pDBLeu and pEXP-AD502 are control constructs lacking inserts for the bait and prey vectors, respectively.

[a] Plates were also lacking Leu and Trp. In addition, His-minus plates contained 75 mM 3AT.

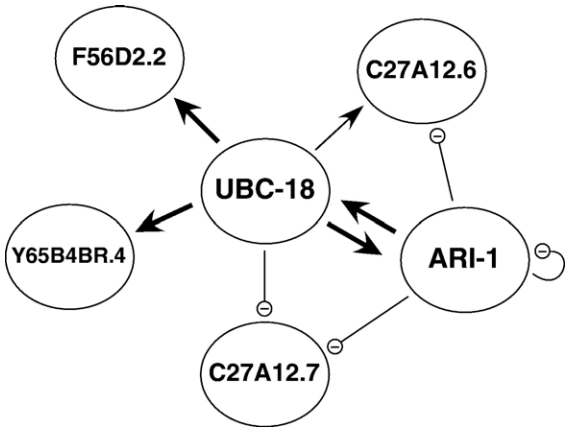

Fig. 1. Summary of physical interactions. Arrows indicate interactions detected using the two- hybrid system. Proteins at the base of the arrow were expressed in the bait configuration, whereas proteins at the tip were in prey configuration. Thick arrows indicate the activation of all three reporter genes (*HIS3*, *URA3*, and *lacZ*); thin arrows, HIS3 only. Circles with negative signs indicate that no reporter genes were activated. For additional details, see Table 1 and text.

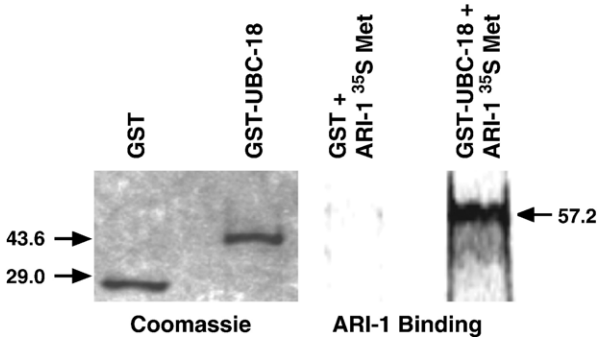

Fig. 2. In vitro interaction of UBC-18 and ARI-1. A bacterially produced GST–UBC-18 fusion protein along with control GST alone were tested for interactions with ^{35}S-Met radiolabeled ARI-1 to independently confirm the physical interaction found by yeast two-hybrid assays. Full-length radiolabeled ARI-1 was synthesized using TNT T7 Quick for PCR DNA (Promega) and tested for its capacity to form a stable complex with GST alone and GST fused to full-length UBC-18 (GST–UBC-18). Left two lanes show Coomassie staining of the purified GST and GST–UBC-18 proteins. Right two lanes show the corresponding autoradiograph following incubation with ^{35}SMet ARI-1. Expected sizes for the GST, GST–UBC-18, and ARI-1 protein are 29 kDa, 43.6 kDa, and 57.2, kDa, respectively. Arrows indicate expected migration positions based on standard markers. Also see Materials and methods.

To determine the regions of ARI-1 required for binding UBC-18, we tested several additional N-terminal deletion constructs using the two-hybrid assay (Δ123 and Δ178) and found that the removal of sequences up to and including the first RING finger of ARI-1 (aa 128–174) was sufficient to abrogate binding to UBC-18 (Table 1). This is consistent with previous studies showing a requirement for the first RING finger of human and *Drosophila* Ariadne proteins in binding to ubiquitin-conjugating enzymes (Aguilera et al., 2000; Moynihan et al., 1999), but also indicates a significant contribution of sequences N-terminal to the first RING finger for this interaction in *C. elegans*. We also found that under our assayed conditions, a region of ARI-1 spanning the N-terminal RING finger up to the start of the IBR domain (43–191; the IBR domain encompasses aa 196–256) was not sufficient for binding UBC-18 (Table 1). This is consistent with in vitro studies on the human Ariadne protein demonstrating a requirement for N-terminal IBR domain sequences for this interaction (Moynihan et al., 1999), but differs from two-hybrid findings for *Drosophila* ARI-1 (Aguilera et al., 2000). These partially conflicting results may reflect authentic differences in the binding properties of the various ARI-1 orthologs or may be due to differences in the assay methods used (including differences in the yeast strains, expression plasmids, and reporters).

ARI-1 acts with UBC-18 to regulate pharyngeal development

To determine if one or more of the identified putative ligases function with UBC-18 in controlling pharyngeal development, we assayed for the presence of the Pharynx Unattached (Pun) phenotype in larvae and embryos from *pha-1(e2123)* mutants (at the permissive temperature of 16°C) that we treated with dsRNA against each of the three putative ligases (using RNAi feeding). Strikingly, *ari-1* produced a high percentage of Pun animals in this background at levels that were effectively indistinguishable from that of *ubc-18(RNAi)* (Table 2 and Fig. 3; Fay et al., 2004). Furthermore, like *pha-1; ubc-18(RNAi)* mutants, the pharynges of *pha-1; ari-1(RNAi)* mutants failed to achieve proper attachment with the anterior buccal cavity but nevertheless underwent proper differentiation of tissues such as muscle and epithelium (Fig. 3 and data not shown). In contrast, inactivation of *wwp-1* and F56D2.2 failed to produce a Pun phenotype in this background, suggesting that these ligases may function with UBC-18 to control other aspects of development (Table 2). We also note that none of the three ligases tested by RNAi displayed any obvious phenotype in the wild-type background (also see below).

We further tested for the ability of *ari-1(RNAi)* to enhance the Pun phenotype of *lin-35; ubc-18* double mutants. Because *ubc-18(ku354)* is a partial loss-of-function (LOF) allele, a further reduction in the activity of the relevant E3 ligase would be expected to enhance the penetrance of the Pun phenotype in this sensitized background (Fay et al., 2003). Consistent with ARI-1 acting as the downstream ligase, similar high numbers of Pun larvae were observed following reduction of *ari-1* or *ubc-18* by RNAi in the double-mutant background (Table 2). Also similar to *ubc-18*, inactivation of *ari-1* by RNAi in the *lin-35* single-mutant background failed to produce defects, presumably due to limitations of RNAi (Table 2; Fay et al., 2003). We have also previously shown that two suppressors of strong *pha-1* LOF mutations [*sup-36(e2217)* and *sup-37(e2215)*] (Schnabel et al., 1991) are capable of suppressing the synthetic lethality of *pha-1; ubc-18* and *lin-35; ubc-18* double mutants (Fay et al., 2004). Similarly, both mutations suppressed the ability of *ari-1 (RNAi)* to enhance the Pun phenotype of *pha-1(e2123)* mutants at 16°C (Table 2).

Table 2
Genetic interactions of *ari-1*

Strain	% Pun
N2 [a]	0 (n = 260)
pha-1(e2123) [b]	0 (n = 189)
pha-1; ubc-18(RNAi) [b]	77 (n = 62)
pha-1; ari-1(RNAi)	76 (n = 203)
pha-1; F56D2.2(RNAi)	0 (n = 136)
pha-1; wwp-1(RNAi)	0 (n = 158)
pha-1; sup-36(e2217); ubc-18(RNAi)	0 (n = 83)
pha-1; sup-37(e2215); ubc-18(RNAi)	0 (n = 64)
pha-1; sup-36; ari-1(RNAi)	0 (n = 101)
pha-1; sup-37; ari-1(RNAi)	0 (n = 133)
lin-35(n745) [a]	0 (n = 268)
ubc-18(ku354) [a]	0 (n = 101)
ubc-18(RNAi) [a]	0 (n = 100)
lin-35; ubc-18 [a]	4 (n = 192)
lin-35; ubc-18; ubc-18(RNAi) [a]	40 (n = 174)
lin-35; ubc-18(RNAi) [a]	0 (n = 255)
ari-1(RNAi)	0 (n = 80)
lin-35; ubc-18; ari-1(RNAi)	43 (n = 88)
lin-35; ari-1(RNAi)	0 (n = 126)

RNAi experiments were conducted by feeding methods (see Materials and methods). RNAi of *ari-1* targeted the central coding regions of the indicated genes (also see Table 3 and Materials and methods). Experiments with *pha-1* mutants were conducted at 16°C. All other experiments were conducted at 20°C.
[a] From Fay et al. (2003).
[b] From Fay et al. (2004).

The observation that inactivation of *ubc-18* or *ari-1* in *pha-1* and *lin-35; ubc-18* mutant backgrounds produces nearly identical results suggests that ARI-1 may be the exclusive partner of UBC-18 in pharyngeal development and vice versa (also see below). This suggestion is consistent with our observation that in a large-scale two-hybrid screen using ARI-1 as bait (~2 × 10^6 colonies), we isolated seven independent clones of UBC-18 but failed to identify any other ubiquitin-conjugating enzymes (X. Q. and D. F. unpublished results). Taken together, these data strongly support the model that ARI-1 acts with UBC-18 to control pharyngeal development through a pathway that is genetically redundant with both *lin-35* and *pha-1*.

ARI-1 is a member of the RBR family of E3 ligases

ari-1 encodes a 494-amino-acid protein that is a member of the Ariadne subfamily of RBR ligases. RBR ligases are characterized by an IBR/DRIL domain that is flanked by two RING fingers motifs (Marin et al., 2004). The IBR/DRIL domain is composed of a cysteine-rich C_6HC pattern, whereas the RING fingers are distinguished by a C_3HC_4 signature (Fig.

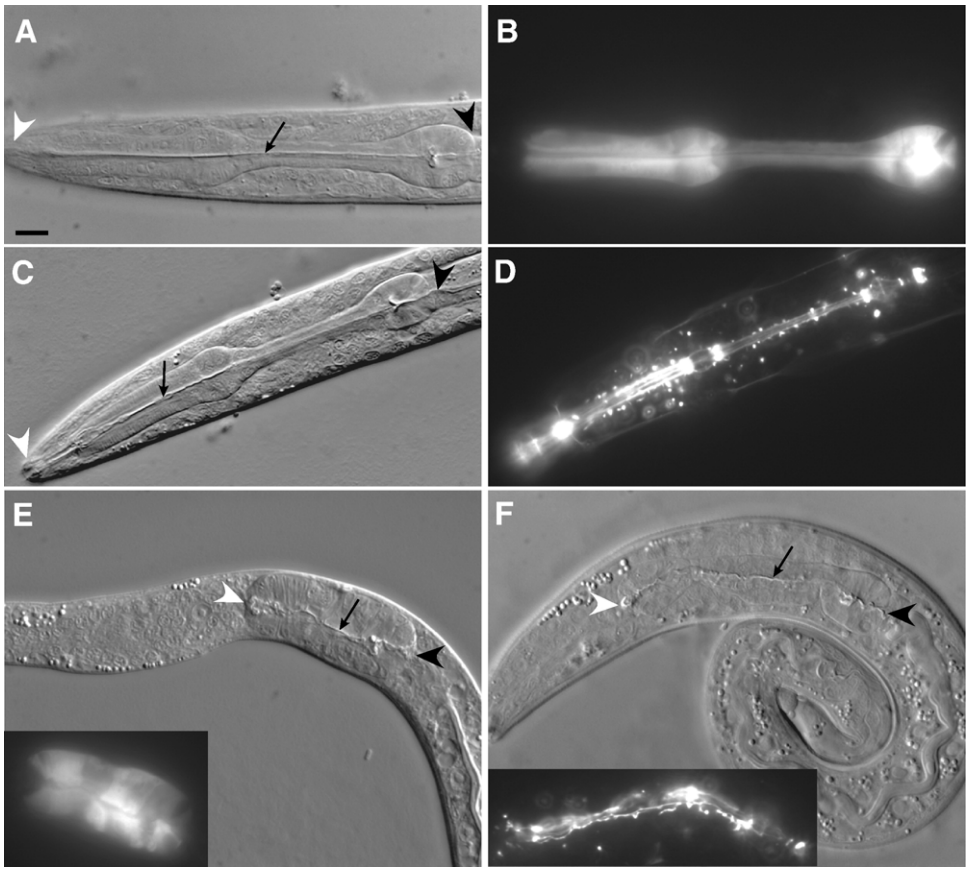

Fig. 3. Pharyngeal defects of *pha1; ari1(RNAi)* mutants. Corresponding DIC (A, C, E, F) and GFP (B, D; E and F, insets) images of L1 larvae of *pha-1(e2123)* (A–D) and *pha-1; ari-1(RNAi)* mutants (E, F) at 16°C. Larvae in panels A and E express a MYO-2: :GFP reporter that is specific to differentiated pharyngeal muscle. The larvae in panels C and F express AJM-1: :GFP, which is a marker of adherens junctions and differentiated epithelial tissue. White and black arrowheads denote anterior and posterior pharyngeal boundaries, respectively; black arrow indicates the pharyngeal lumen. Note the presence of a lumen and the strong expression of the muscle and epithelial markers in the affected mutant pharynges. Scale bar in panel A, 10 μm for panels A–D.

4A). In addition to the RBR motif, the Ariadne subfamily contains an additional ARIADNE domain that is located just C-terminal to the RBR domain. Although the significance of this domain is currently unknown, its existence predates the origin of plants, animals, and fungi (Marin and Ferrus, 2002). Interestingly, a number of RBR family members including Parkin, Dorfin, and the *Drosophila* ARI-1 protein have been found to interact with the corresponding orthologs of UBC-18 in other species, indicating that this interaction has been evolutionarily conserved (Aguilera et al., 2000; Niwa et al., 2001; Shimura et al., 2000). Consistent with these findings, a second ligase identified by our screen, F56D2.2, is a member of the ARA54 subfamily of RBR proteins.

The *C. elegans* genome encodes five bona fide *ariadne* family members including two genes (C27A12.6 and C27A12.7) that are immediately adjacent to *ari-1* on chromosome I. Based on an alignment with the corresponding region from *C. briggsae*, this gene duplication event predates the separation of these species (~23–40 million years; Gupta and Sternberg, 2003). ARI-1 is 76% identical to C27A12.6 and 75% identical to C27A12.7 at the amino acid level and is ~75% identical to both genes at the mRNA level (C27A12.6 and C27A12.7 are 73% identical at the amino acid level; Fig. 4 and data not shown). The ARI-1 protein is also 60% identical to Y73F8A.34 and 30% identical to T12E12.1, the later protein being more closely related to the ARI-2 protein from other species (Fig. 4 and data not shown). We also note the existence of what appears to be a partial duplication of gene Y73F8A.34. This sequence is currently annotated as a predicted gene (C17H11.4) but lacks confirmation by cDNAs and is not present in *C. briggsae*. The complete predicted C17H11.4 protein is 91% identical at the amino acid level to Y73F8A.34 residues 359–467 but is missing an N-terminal domain containing the RING and IBR motifs. These observations, coupled with the absence of any suggestion of an N-terminal domain based on the upstream genomic sequence, suggest that C17H11.4 may be a pseudogene. Lastly, an additional (though highly divergent) family member may be represented by Y57A10A.31; Y57A10A.31 shows ~25% identity to other *C. elegans* Ariadne family members within the RBR domain but lacks the signature Ariadne C-terminal motif (data not shown).

Analysis of ariadne family members in C. elegans

We tested the four other *ariadne* family members in *C. elegans* for their ability to enhance the Pun phenotype of *pha-1 (e2123)* and *lin-35; ubc-18* mutants. As shown in Table 3, RNAi of the approximate “central coding regions” of both C27A12.6

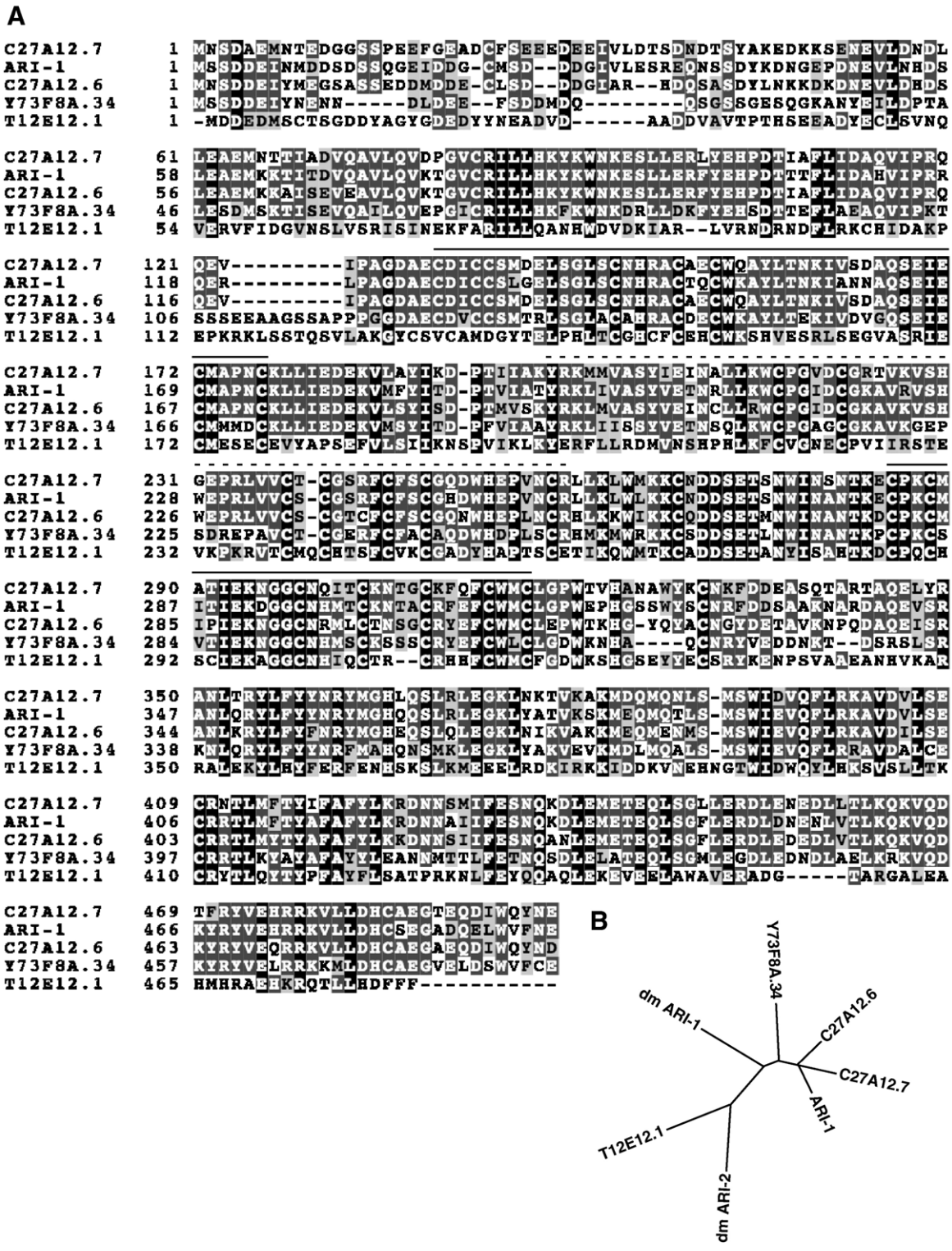

Fig. 4. Alignment of *ariadne* family members in *C. elegans*. (A) Peptide alignment of *C. elegans ariadne* members using Clustal W. The location of the two RING fingers are indicated by the solid bars; overhead dashed line indicates the location of the IBR/DRIL domain. Black boxes indicate residues conserved in all proteins; dark gray, identities; light gray, similarity. (B) Phylip-format dendrogram (unrooted) showing relatedness of *C. elegans* and *D. melanogaster* (dm) Ariadne family members.

and C27A12.7 resulted in a substantial increase in the percentage of Pun animals in both mutant backgrounds (but not in N2), although the effect was markedly less than that observed for *ari-1* (for a precise definition of the "central coding regions" targeted by these constructs see Materials and methods). In contrast, the more distantly related *ariadne* family members Y73F8A.34 and T12E12.1 produced little or no effect in either background (Table 3). We also note that we failed to

Table 3
Genetic interactions of *ariadne* family members

Strain	% Pun
N2 [a]	0 (n = 260)
ari-1(RNAi) [b, c]	0 (n = 80)
C27A12.6(RNAi) [b, c]	0 (n = 166)
C27A12.7(RNAi) [b, c]	0 (n = 124)
Y73F8A.34(RNAi) [b, c]	0 (n = 123)
T12E12.1(RNAi) [b, c]	0 (n = 113)
pha-1(e2123) [d]	0 (n = 189)
pha-1; ari-1(RNAi) [c]	76 (n = 203)
pha-1; C27A12.6(RNAi) [c]	34 (n = 85)
pha-1; C27A12.7(RNAi) [c]	38 (n = 52)
pha-1; Y73F8A.34(RNAi) [c]	0 (n = 142)
pha-1; T12E12.1(RNAi) [c]	1 (n = 117)
lin-35; ubc-18 [a]	4 (n = 192)
lin-35; ubc-18; ubc-18(RNAi) [a]	40 (n = 174)
lin-35; ubc-18; ari-1(RNAi) [c]	43 (n = 88)
lin-35; ubc-18; C27A12.6(RNAi) [c]	35 (n = 88)
lin-35; ubc-18; C27A12.7(RNAi) [c]	27 (n = 122)
lin-35; ubc-18; Y73F8A.34(RNAi) [c]	10 (n = 56)
lin-35; ubc-18; T12E12.1(RNAi) [c]	2 (n = 61)
pha-1; ari-1–3′UTR(RNAi) [e]	9 (n = 298)
pha-1; C27A12.6–3′UTR(RNAi) [e]	0 (n = 133)
pha-1; C27A12.7–3′UTR(RNAi) [e]	0 (n = 124)
lin-35; ubc-18; ari-1–3′UTR(RNAi) [e]	55 (n = 126)
lin-35; ubc-18; C27A12.6–3′UTR(RNAi) [e]	19 (n = 173)
lin-35; ubc-18; C27A12.7–3′UTR(RNAi) [e]	20 (n = 179)
pha-1; ari-1–5′(RNAi) [f]	11 (n = 299)
pha-1; C27A12.6–5′(RNAi) [f]	1 (n = 214)
pha-1; C27A12.7–5′(RNAi) [f]	1 (n = 318)
lin-35; ubc-18; ari-1–5′(RNAi) [f]	26 (n = 127)
lin-35; ubc-18; C27A12.6–5′(RNAi) [f]	10 (n = 79)
lin-35; ubc-18; C27A12.7–5′(RNAi) [f]	14 (n = 48)

Experiments with *pha-1* mutants were conducted at 16°C. All other experiments were conducted at 20°C. All experiments were conducted by RNAi feeding methods. For ease of comparison, several data points shown in Table 2 have been reproduced in this table. Also see Materials and methods.

[a] From Fay et al. (2003).

[b] Identical results were also obtained by RNAi injection methods. In all experiments, no obvious morphological defects were observed.

[c] Constructs targeted the central coding regions of the indicated genes.

[d] From Fay et al. (2004).

[e] Constructs targeted the 3′UTR regions of indicated genes (excluding the 100 bp region directly following the termination codon).

[f] Constructs targeted the 5′ coding regions of indicated genes.

observe any defects in the progeny of animals injected with dsRNAs against the five individual *ariadne* family members (using wild-type and the RNAi hypersensitive strain *rrf-3*; Simmer et al., 2002), nor were defects detected following combinatorial injections of dsRNAs (data not shown, also see Materials and methods). Nevertheless, because RNAi can be insufficient to fully inactivate gene function, it remains possible that one or more *ariadne* family members may carry out essential functions.

The ability of ARI-1, C27A12.6, and C27A12.7 to enhance the Pun phenotype in the mutant strains could reflect a redundant role for all three proteins in pharyngeal development or might be the result of RNAi cross-reactivity (also known as off-target silencing) given the extensive homology between these genes at the mRNA level. In fact, an examination of the coding regions targeted by these constructs revealed a 20-bp stretch of contiguous identity between *ari-1* and C27A12.7 and three stretches of contiguous identity (20–32 bp) between *ari-1* and C27A12.6 (also see Materials and methods). In addition, a number of smaller stretches of contiguous identity (in the range of 11–17 bp) are also present (data not shown). To directly test for RNAi cross-reactivity, we carried out RNAi experiments in strains that express a full-length ARI-1::GFP fusion protein (also see below). In the event of cross-reactivity by the *ari-1* paralogs, we would expect to see a reduction in the intensity of ARI-1::GFP fluorescence in the treated animals. In fact, we observed a consistent and significant reduction in ARI-1::GFP expression when strains were treated with RNAi against the central coding regions of C27A12.6 and C27A12.7, although the reduction in expression was notably less than that observed for RNAi of *ari-1* (Fig. 5). This result suggests that the enhancement of the Pun phenotype by C27A12.6 and C27A12.7 may for the most part be due to off-target silencing effects as opposed to a role for these proteins in pharyngeal development.

To further examine the relative contributions of C27A12.6, C27A12.7, and *ari-1* in pharyngeal development, we carried out RNAi experiments in which we targeted the more variable 5′ coding regions and the highly divergent 3′ UTRs of these genes (Table 3; also see Materials and methods). As shown in Fig. 5 and Table 3, although some cross-reactivity with *ari-1* was observed for all the constructs tested, substantially stronger phenotypic effects were generated within each class using the RNAi constructs directed against *ari-1*. We note that in some cases there did not appear to be a perfect correlation between the levels of RNAi knockdown in the reporter strain (based on GFP intensity) versus the sensitized backgrounds (based on the percentage of Pun animals). These differences are likely to reflect some pleiotropy present within the tester strains, experimental variability inherent in the RNAi knockdown experiments, and possible differences in the efficiency of RNAi knockdown between the overexpressed ARI-1::GFP reporter and the endogenous gene. The ability of the 5′ and 3′ RNAi constructs of C27A12.6 and C27A12.7 to cross-react with *ari-1* is likely due to several 10- to15-bp stretches of mRNA identity within the 5′ coding regions of these genes and to the effects of transitive RNAi, respectively (Alder et al., 2003; Jackson et al., 2003; Sijen et al., 2001).

Taken together, the above results are consistent with the model that ARI-1 is the primary, if not exclusive, *ariadne* family member involved in the redundant control of pharyngeal development with UBC-18. In further support of this, we found that simultaneous inactivation of multiple family members did not enhance the frequency of defects in the sensitized strains beyond what was observed for knockdown using RNAi constructs targeting *ari-1* alone (data not shown). In addition, C27A12.7 failed to interact with UBC-18 in two-hybrid tests, whereas C27A12.6 showed only very weak interactions with UBC-18, raising the possibility that these proteins may not function with UBC-18 in vivo (Table 1). Moreover, we found no evidence for dimerization of ARI-1 either with itself (as was previously reported for the *Drosophila* ARI-1 ortholog; Aguilera et al., 2000) or with C27A12.6 or

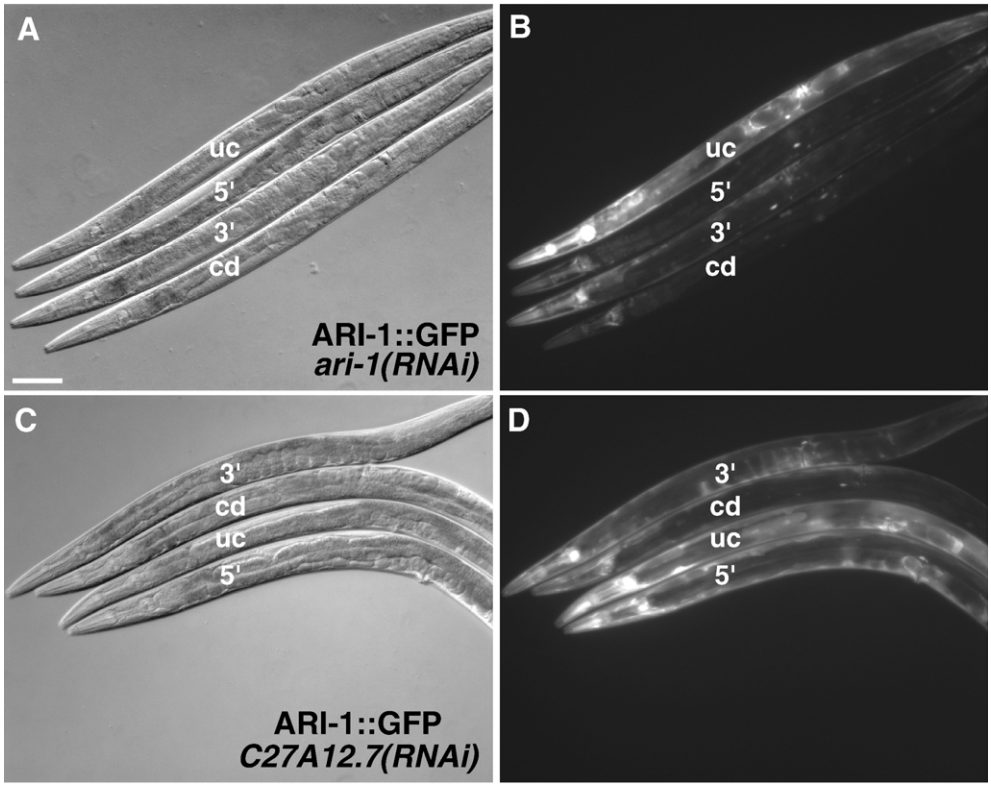

E

RNAi	ARI-1::GFP intensity
Untreated control	++++++
ari-1 central coding	+
ari-1 5' coding	++
ari-1 3'UTR	+++
C27A12.6/7 central coding	+++
C27A12.6/7 5' coding	+++++
C27A12.6/7 3'UTR	++++

Fig. 5. Off-target RNAi silencing of *ari-1* by paralogs. DIC (A, C) and corresponding GFP (B, D) images of strain WY246, which expresses an integrated full-length ARI-1: :GFP fusion protein under the control of the *ari-1* promoter. Effects of ARI: :GFP expression following RNAi treatment (by feeding) using constructs directed against *ari-1* (A, B) and C27A12.7 (C, D) are shown. uc, untreated control; cd, RNAi constructs targeting the central coding regions; 5′, RNAi constructs targeting the more divergent 5′ coding regions; 3′, RNAi constructs targeting the highly divergent 3′UTRs. (E) Summary of results for all RNAi constructs tested. The average relative GFP intensities for each condition tested are indicated (++++++, strongest; + weakest). The corresponding constructs for C27A12.6 and C27A12.7 gave identical results.

C27A12.7 (Table 1). Still, our cumulative results cannot rule out the possibility of a minor role (relative to ARI-1) for one or both family members in the regulation of pharyngeal development; we note that LOF alleles for *ari-1* and its paralogs in *C. elegans* do not currently exist.

ARI-1 expression during development

To examine the pattern of ARI-1 expression in living animals, we generated two expression vectors, each containing the full-length *ari-1* gene and associated regulatory elements fused to GFP at either the N or C terminus of the coding regions (also see Materials and methods). Both N- and C-terminal fusions gave identical patterns of expression, indicating that the chimeric peptide is likely to reflect the expression pattern associated with the endogenous ARI-1 protein (data not shown). Expression of ARI-1 is dynamic during early embryonic development, with ubiquitous somatic expression occurring between the 50- and 200-cell stage (Figs. 6A, B). By the late proliferative phase of embryogenesis (~400–500 cells), expression is reduced in most nuclei but is maintained at high levels in muscle precursors (Figs. 6C, D). Similar to later embryonic and larval time points, expression in the early embryo is always observed in both the nucleus and cytoplasm of GFP-positive cells. Consistent with this observation, sequence analysis of ARI-1 using PSORT predicts ARI-1 to be a nuclear protein.

Following the proliferative phase of embryogenesis, ARI-1 embryonic expression is most pronounced in muscle precursors with moderate expression also occurring in the lateral ectoderm, which gives rise to many neurons in addition to hypodermal

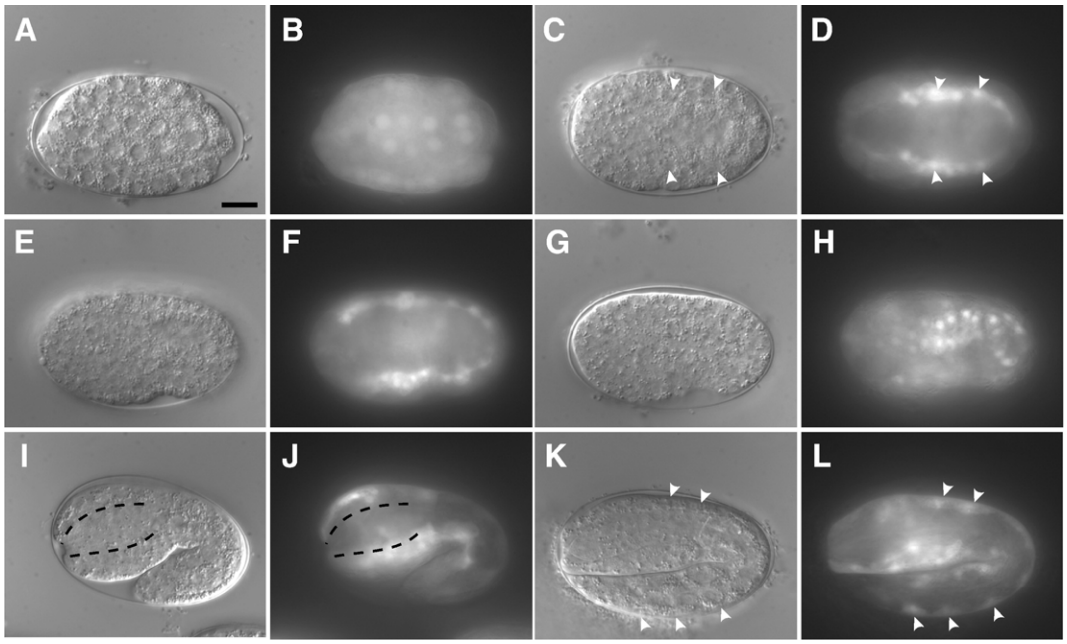

Fig. 6. ARI-1: :GFP expression in embryos. DIC (A, C, E, G, I, K) and corresponding GFP (B, D, F, H, J, L) images of strain WY246, which expresses an integrated full-length ARI-1: :GFP fusion protein under the control of the *ari-1* promoter. White arrowheads indicate muscle and muscle cell precursors; black dashed lines in panels I and J indicate the approximate region of the developing pharynx. Anterior is to the left. (A, B) ~50-cell-stage embryo. (C, D) ~400-cell-stage embryo. (E–H) Post-proliferative lima bean stage embryo (~550 cells) with views through the middle (E, F) and lateral (G, H) focal planes. Note the expression in presumptive ectodermal cells in the lateral projection. 1.5-fold-stage (I, J) and 2-fold-stage (K, L) embryos with primary expression observed in muscle progenitors. Note the relative absence of ARI-1 expression in the foregut region of the 1.5-fold-stage embryo. For further details, see text. Scale bar in panel A, 10 μm for panels A–L.

cells (Figs. 6E–L). Notably, pharyngeal expression of ARI-1 is very low at both the comma and 1.5-fold embryonic stages (Figs. 6I, J, and data not shown), during which time pharyngeal morphogenesis and attachment are occurring. This raises the possibility that ARI-1 may act nonautonomously to control pharyngeal development or may reflect the need for only low levels of ARI-1 in the pharyngeal precursor cells undergoing morphogenesis. Alternatively, higher levels of ARI-1 may be required in pharyngeal precursor cells during an earlier developmental stage in order for proper pharyngeal development to occur later.

Consistent with the embryonic expression pattern, ARI-1 is present at highest levels in muscle and neuronal cells in larvae and adults. Expression in muscle cells is observed at all stages including the body wall muscles (Figs. 7A, B), sex muscles (Figs. 7C, D), muscles associated with the posterior alimentary tract (Figs. 7E, F), and in lateral head and pharyngeal muscles (Figs. 7M, N). In addition, we observed consistent expression in a number of cells of the somatic gonad including distal tip, sheath, and spermathecal cells, as well as in vulval cells undergoing morphogenesis (Figs. 7A, B, G–J). Expression is also observed in head neurons, including many of the amphid neurons that are proximal to the posterior bulb of the pharynx (Figs. 7M–P) and in neurons in the tail including DVA, DVB, and DVC (data not shown). Neuronal expression in the mid-body includes the CAN, HSN, and ALM cells; neurons of the ventral and dorsal cords; and a number of posterior deirid neurons (Figs. 7A, B, K, L, and data not shown). Lastly, expression is observed in all pairs of coelomocytes (Figs. 7K, L, and data not shown).

We also attempted to assay for the presence of ARI-1: :GFP in the hermaphrodite germline using low-copy integrants obtained through microparticle bombardment (Praitis et al., 2001). Although several such lines were obtained, expression levels proved too low for reliable detection in any tissue (data not shown). We therefore carried out in situ hybridization to

Fig. 7. ARI-1: :GFP expression in larvae and adults. DIC (A, C, E, G, I, K, M, O) and corresponding GFP (B, D, F, H, J, L, N, P) images of hermaphrodites from strains WY222 (C, D, K, L) and WY246 (all other panels), which express full-length ARI-1: :GFP fusion proteins under the control of the *ari-1* promoter. Anterior is to the left and ventral is down unless otherwise indicated. (A, B) L2 larva showing expression in body wall muscles (white arrowheads) and the CAN neuron, black arrowhead; white arrow indicates a distal tip cell. (C, D) Young adult (ventral side up) showing expression in the vulval muscles vm1 and vm2 (white arrowheads); white arrow indicates the vulval lumen. (E, F) Tail region of an L1 larva showing expression in the anal sphincter muscle (black arrowheads), anal depressor muscle (white arrow), and the intestinal muscle (white arrowhead). (G, H) L4 larva showing expression in the distal tip cell (black arrowhead main panel), gonadal sheath cells (white arrowheads), and cells in the region of the developing spermatheca (white bracket). Inset shows expression in the vulva in a mid-stage L4 larva; black arrowheads indicate the positions of vulval muscle cell nuclei. (I, J) Expression in the adult spermatheca. (K, L) Young adult showing expression in the CAN neuron and processes (white arrowhead), the HSN neuron (black arrowhead), and two coelomocytes (black arrows). Central (M, N) and lateral (O, P) focal-plane views of head region of an L2 (M, N) and L1 (O, P) larva showing expression in head muscles (white arrowheads) and neurons (black arrowheads). The cells indicated by the black arrowheads (M–P) are most likely amphid neurons. The white brackets (M–P) indicate the position of the posterior pharyngeal bulb. (Q, R) In situ hybridization using control sense (Q) and antisense (R) probes for *ari-1*. White arrows indicate equivalent regions in the germlines of control and experimental hermaphrodites. Scale bar in panel A, 10 μm for panels A, B, G, H, Q, R; in panel C, 10 μm for panels C–F, I, J, M–P, and panels G and H insets; in panel K, 10 μm for panels K, L.

examine *ari-1* mRNA levels directly in the germline. Our results indicate that *ari-1* is consistently expressed in the germline of adults and larvae (Figs. 7Q, R, and data not shown). We note, however, that levels of *ari-1* mRNA were relatively modest compared to that of a positive control that is expressed at high levels in this tissue (*hmg-3*, data not shown).

Discussion

We have demonstrated a role for the RBR family ubiquitin-ligase ARI-1 in the control of pharyngeal development with UBC-18 (see Results and Fay et al., 2003). Our data also strongly suggest that ARI-1 is the principal, if not exclusive,

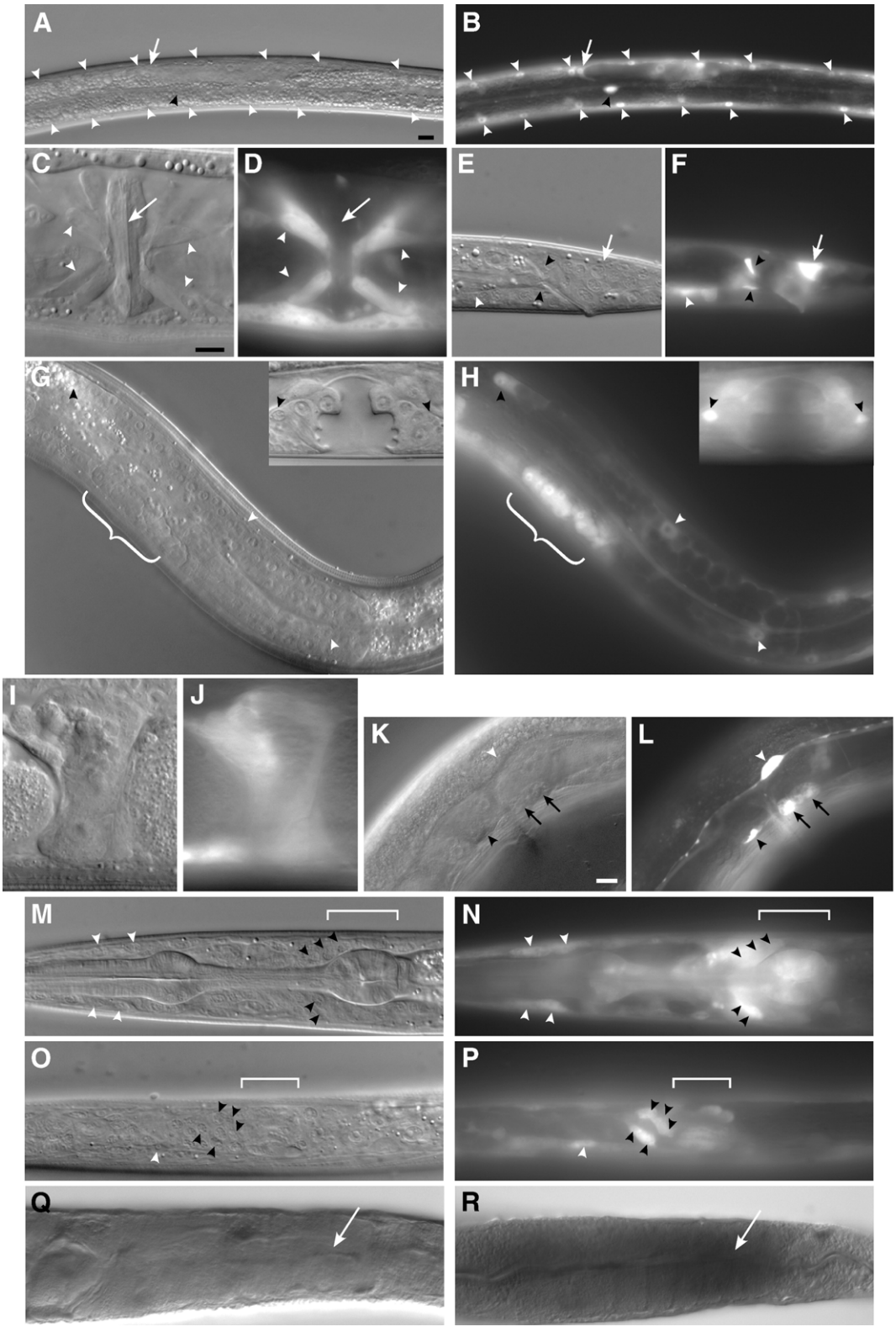

partner of UBC-18 in this process. While a number of previous studies have reported physical interactions between paralogs of UBC-18 and RBR-family ligases (Aguilera et al., 2000; Ardley et al., 2001; Martinez-Noel et al., 1999; Shimura et al., 2000), our findings demonstrate that these proteins are also functionally connected based on in vivo genetic and phenotypic analyses.

Interestingly, a conserved role for Ariadne family proteins in morphogenesis is further supported by studies on the *ari-1* ortholog in *Drosophila* (Aguilera et al., 2000). In *Drosophila*, *ari-1* mutants show pleiotropic defects including abnormal bristles, misrouted axonal tracts, defects in neuronal connectivity, and misshapen tubular muscles. The aberrant bristles were reported to be altered in shape but not in number or pattern. Furthermore, neuronal connectivity phenotypes were suggested to be the result of incorrect decisions or signals affecting leading growth cones as opposed to generalized adhesion defects. The authors concluded that "the cell types in which the mutant phenotypes are most apparent are those that require a massive and rapid membrane deposition". Based on this study, as well as our previous analysis of *lin-35; ubc-18* mutants indicating a defect in cell polarity, shape, and orientation (but not in cell number or differentiation per se; Fay et al., 2003), it seems likely that Ariadne family members may generally regulate aspects of morphogenesis during development through the control of cell shape or polarity.

We also note that an analysis of *ariadne* mRNA expression in *Drosophila* revealed prominent expression in neurons as well as the female somatic gonad, two of the principal tissues in which we observed ARI-1∷GFP expression (Fig. 7; Aguilera et al., 2000). Furthermore, like *Drosophila ari-1*, *C. elegans ari-1* is expressed in the adult germline (Fig. 7). This finding is also consistent with the observed expression of *ubc-18* in germline tissue (based on data available on the *C. elegans* expression pattern database; http://nematode.lab.nig.ac.jp/). Although we were surprised by the relative lack of ARI∷GFP expression in the mid-stage embryonic pharynx (Fig. 6), it is possible that ARI-1 may act nonautonomously to control pharyngeal development, as was recently demonstrated for LIN-35 in the regulation of vulval induction (Myers and Greenwald, 2005). Alternatively, maternal sources (as indicated by *ari-1* mRNA expression in the germline) may be sufficient to drive ARI-1 protein expression in this tissue.

A notable feature of RBR family genes in *C. elegans* (and more generally in *Caenorhabditis* species) is the degree of expansion that has taken place. As discussed above, there are four unambiguous *ari-1*-like genes (plus one probable pseudogene and another related though highly divergent family member) in *C. elegans*, as compared with two in *Drosophila* (Marin and Ferrus, 2002). Expansion in *C. elegans* has also taken place in two other RBR subfamilies, ARA54 and Dorfin (Marin and Ferrus, 2002). In fact, the ARA54 member identified by our two-hybrid screen, F56D2.2, is 66% identical at the peptide level to another family member on the same cosmid, F56D2.5, a duplication event that also predates the separation of *C. elegans* and *C. briggsae* species (data not shown). Thus, in contrast to humans (and most likely insects), selective pressure has led to an expansion of RBR members in at least a subset of nematode species (Marin and Ferrus, 2002).

Our experiments also uncovered a high degree of RNAi cross-reactivity among the *ari-1* paralogs on cosmid C27A12 (Fig. 5). Although these genes are indeed highly homologous at the mRNA level (~75% overall identity), the extent of contiguous identity in excess of 20–22 nucleotides is in fact very limited (Supplementary Figs. 1 and 2). For example, whereas significant cross-reactivity with *ari-1* was observed for the RNAi construct targeting an ~600-bp sequence in the central coding region of C27A12.7, this segment only contains a single stretch of 20 identical nucleotides to the corresponding region of *ari-1*, along with five stretches of 17 nucleotides, and one each of 13 and 14. Based on this limited homology as well as the established mechanism by which dsRNA is processed into ~22-bp fragments and incorporated in the RNAi silencing complex (RISC; Sontheimer, 2005; Zamore et al., 2000), it is therefore very probable that only a small percentage (if any) of the active RISC complexes derived from C27A12.7 would contain 17 or more consecutive nucleotides that are complementary to the *ari-1* mRNA. The situation is similar for the 5′ coding region RNAi constructs of C27A12.6 and C27A12.7, which would produce products that contain at maximum 14–15-bp of contiguous identity to *ari-1*, but nevertheless resulted in low but consistent cross-reactivity.

The above results indicate that 14 or fewer base pairs of contiguous identity are sufficient to cause significant off-target RNAi silencing in *C. elegans*. This finding is consistent with reports in mammals suggesting that as few as 11 contiguous base pairs of identity may be sufficient to result in off-target silencing by siRNAs (Jackson et al., 2003). These findings emphasize that caution must be taken when interpreting RNAi results among genes with close family members. We also note that despite the incorporation of a 100-bp "spacer region" at the 5′ ends of our RNAi constructs targeting the 3′ UTRs of the *ari-1* paralogs, we nevertheless observed significant cross-reactivity to *ari-1* due to transitive RNAi. Thus, although spacers of ~100-bp were previously reported to substantially reduce the effects of transitive RNAi (Alder et al., 2003; Sijen et al., 2001), this may not be sufficient to completely abolish cross-reactivity for many genes.

It will be of significant interest to identify the downstream targets of ARI-1, as well as other Ariadne and RBR family members in *C. elegans*. Future work will also be directed towards elucidating potential additional partners for Ariadne proteins, such as cullins or other proteins that may function in a complex with Ariadne proteins or may be required for their full activation.

Acknowledgments

We thank the *C. elegans* Genetics Consortium and the National Biosource Project for the Experimental Nematode *C. elegans* for strains, Andy Fire for vectors, and Mike Boxem and Yuji Kohara for reagents. We also thank Amy Fluet for editing the manuscript, Iqbal Ahmed and the Thorsness Lab at

UW for technical assistance, and Meera Sundarum, Harold Smith, Saeyoull Cho, Abigail Farfan, and Chris Malone for technical advice. This work was funded by grants from the American Cancer Society and the National Institutes of Health (R01GM066868-02).

Appendix A. Supplementary data

Supplementary data associated with this article can be found in the online version at doi:10.1016/j.bbadis.2005.07.003.

References

Aguilera, M., Oliveros, M., Martinez-Padron, M., Barbas, J.A., Ferrus, A., 2000. Ariadne-1: a vital *Drosophila* gene is required in development and defines a new conserved family of ring-finger proteins. Genetics 155, 1231–1244.

Alder, M.N., Dames, S., Gaudet, J., Mango, S.E., 2003. Gene silencing in *Caenorhabditis elegans* by transitive RNA interference. RNA 9, 25–32.

Ardley, H.C., Tan, N.G., Rose, S.A., Markham, A.F., Robinson, P.A., 2001. Features of the parkin/ariadne-like ubiquitin ligase, HHARI, that regulate its interaction with the ubiquitin-conjugating enzyme. Ubch7. J. Biol. Chem. 276, 19640–19647.

Bryan, B., Cai, Y., Wrighton, K., Wu, G., Feng, X.H., Liu, M., 2005. Ubiquitination of RhoA by Smurf1 promotes neurite outgrowth. FEBS Lett. 579, 1015–1019.

Castro, A., Bernis, C., Vigneron, S., Labbe, J.C., Lorca, T., 2005. The anaphase-promoting complex: a key factor in the regulation of cell cycle. Oncogene 24, 314–325.

Cowan, C.R., Hyman, A.A., 2004. Asymmetric cell division in *C. elegans*: cortical polarity and spindle positioning. Annu. Rev. Cell Dev. Biol. 20, 427–453.

DeRenzo, C., Reese, K.J., Seydoux, G., 2003. Exclusion of germ plasm proteins from somatic lineages by cullin-dependent degradation. Nature 424, 685–689.

Fay, D.S., Keenan, S., Han, M., 2002. fzr-1 and lin-35/Rb function redundantly to control cell proliferation in *C. elegans* as revealed by a nonbiased synthetic screen. Genes Dev. 16, 503–517.

Fay, D.S., Large, E., Han, M., Darland, M., 2003. lin-35/Rb and ubc-18, an E2 ubiquitin-conjugating enzyme, function redundantly to control pharyngeal morphogenesis in *C. elegans*. Development 130, 3319–3330.

Fay, D.S., Qiu, X., Large, E., Smith, C.P., Mango, S., Johanson, B.L., 2004. The coordinate regulation of pharyngeal development in *C. elegans* by lin-35/Rb, pha-1, and ubc-18. Dev. Biol. 271, 11–25.

Feng, H., Zhong, W., Punkosdy, G., Gu, S., Zhou, L., Seabolt, E.K., Kipreos, E. T., 1999. CUL-2 is required for the G1-to-S-phase transition and mitotic chromosome condensation in *Caenorhabditis elegans*. Nat. Cell Biol. 1, 486–492.

Fire, A., Xu, S., Montgomery, M.K., Kostas, S.A., Driver, S.E., Mello, C.C., 1998. Potent and specific genetic interference by double-stranded RNA in *Caenorhabditis elegans*. Nature 391, 806–811.

Fraser, A.G., Kamath, R.S., Zipperlen, P., Martinez-Campos, M., Sohrmann, M., Ahringer, J., 2000. Functional genomic analysis of *C. elegans* chromosome I by systematic RNA interference. Nature 408, 325–330.

Furuta, T., Tuck, S., Kirchner, J., Koch, B., Auty, R., Kitagawa, R., Rose, A.M., Greenstein, D., 2000. EMB-30: an APC4 homologue required for metaphase-to-anaphase transitions during meiosis and mitosis in *Caenorhabditis elegans*. Mol. Biol. Cell 11, 1401–1419.

Glickman, M.H., Ciechanover, A., 2002. The ubiquitin-proteasome proteolytic pathway: destruction for the sake of construction. Physiol. Rev. 82, 373–428.

Golden, A., Sadler, P.L., Wallenfang, M.R., Schumacher, J.M., Hamill, D.R., Bates, G., Bowerman, B., Seydoux, G., Shakes, D.C., 2000. Metaphase to anaphase (mat) transition-defective mutants in *Caenorhabditis elegans*. J. Cell Biol. 151, 1469–1482.

Gupta, B.P., Sternberg, P.W., 2003. The draft genome sequence of the nematode *Caenorhabditis briggsae*, a companion to *C. elegans*. Genome Biol. 4, 238.

Hatakeyama, S., Nakayama, K.I., 2003. U-box proteins as a new family of ubiquitin ligases. Biochem. Biophys. Res. Commun. 302, 635–645.

Hicke, L., 2001. Protein regulation by monoubiquitin. Nat. Rev., Mol. Cell Biol. 2, 195–201.

Hubbard, E.J., Wu, G., Kitajewski, J., Greenwald, I., 1997. sel-10, a negative regulator of lin-12 activity in *Caenorhabditis elegans*, encodes a member of the CDC4 family of proteins. Genes Dev. 11, 3182–3193.

Jackson, A.L., Bartz, S.R., Schelter, J., Kobayashi, S.V., Burchard, J., Mao, M., Li, B., Cavet, G., Linsley, P.S., 2003. Expression profiling reveals off-target gene regulation by RNAi. Nat. Biotechnol. 21, 635–637.

Kahle, P.J., Haass, C., 2004. How does parkin ligate ubiquitin to Parkinson's disease? EMBO Rep. 5, 681–685.

Kamath, R.S., Fraser, A.G., Dong, Y., Poulin, G., Durbin, R., Gotta, M., Kanapin, A., Le Bot, N., Moreno, S., Sohrmann, M., Welchman, D.P., Zipperlen, P., Ahringer, J., 2003. Systematic functional analysis of the *Caenorhabditis elegans* genome using RNAi. Nature 421, 231–237.

Kipreos, E.T., Pagano, M., 2000. The F-box protein family. Genome Biol. 1, 1–7.

Kipreos, E.T., Lander, L.E., Wing, J.P., He, W.W., Hedgecock, E.M., 1996. cul-1 is required for cell cycle exit in *C. elegans* and identifies a novel gene family. Cell 85, 829–839.

Kipreos, E.T., Gohel, S.P., Hedgecock, E.M., 2000. The *C. elegans* F-box/WD-repeat protein LIN-23 functions to limit cell division during development. Development 127, 5071–5082.

Kitada, T., Asakawa, S., Hattori, N., Matsumine, H., Yamamura, Y., Minoshima, S., Yokochi, M., Mizuno, Y., Shimizu, N., 1998. Mutations in the parkin gene cause autosomal recessive juvenile parkinsonism. Nature 392, 605–608.

Kitagawa, R., Law, E., Tang, L., Rose, A.M., 2002. The Cdc20 homolog, FZY-1, and its interacting protein, IFY-1, are required for proper chromosome segregation in *Caenorhabditis elegans*. Curr. Biol. 12, 2118–2123.

Kurz, T., Pintard, L., Willis, J.H., Hamill, D.R., Gonczy, P., Peter, M., Bowerman, B., 2002. Cytoskeletal regulation by the Nedd8 ubiquitin-like protein modification pathway. Science 295, 1294–1298.

Levitan, D.J., Boyd, L., Mello, C.C., Kemphues, K.J., Stinchcomb, D.T., 1994. par-2, a gene required for blastomere asymmetry in *Caenorhabditis elegans*, encodes zinc-finger and ATP-binding motifs. Proc. Natl. Acad. Sci. U. S. A. 91, 6108–6112.

Liao, E.H., Hung, W., Abrams, B., Zhen, M., 2004. An SCF-like ubiquitin ligase complex that controls presynaptic differentiation. Nature 430, 345–350.

Marin, I., Ferrus, A., 2002. Comparative genomics of the RBR family, including the Parkinson's disease-related gene parkin and the genes of the ariadne subfamily. Mol. Biol. Evol. 19, 2039–2050.

Marin, I., Lucas, J.I., Gradilla, A.C., Ferrus, A., 2004. Parkin and relatives: the RBR family of ubiquitin ligases. Physiol. Genomics 17, 253–263.

Martinez-Noel, G., Niedenthal, R., Tamura, T., Harbers, K., 1999. A family of structurally related RING finger proteins interacts specifically with the ubiquitin-conjugating enzyme UbcM4. FEBS Lett. 454, 257–261.

Mello, C.C., Kramer, J.M., Stinchcomb, D., Ambros, V., 1991. Efficient gene transfer in *C. elegans*: extrachromosomal maintenance and integration of transforming sequences. EMBO J. 10, 3959–3970.

Mochii, M., Yoshida, S., Morita, K., Kohara, Y., Ueno, N., 1999. Identification of transforming growth factor-beta-regulated genes in *Caenorhabditis elegans* by differential hybridization of arrayed cDNAs. Proc. Natl. Acad. Sci. U. S. A. 96, 15020–15025.

Morett, E., Bork, P., 1999. A novel transactivation domain in parkin. Trends Biochem. Sci. 24, 229–231.

Moynihan, T.P., Ardley, H.C., Nuber, U., Rose, S.A., Jones, P.F., Markham, A. F., Scheffner, M., Robinson, P.A., 1999. The ubiquitin-conjugating enzymes UbcH7 and UbcH8 interact with RING finger/IBR motif-containing domains of HHARI and H7-AP1. J. Biol. Chem. 274, 30963–30968.

Myers, T.R., Greenwald, I., 2005. lin-35 Rb acts in the major hypodermis to oppose ras-mediated vulval induction in *C. elegans*. Dev. Cell 8, 117–123.

Nayak, S., Santiago, F.E., Jin, H., Lin, D., Schedl, T., Kipreos, E.T.,

2002. The *Caenorhabditis elegans* Skp1-related gene family: diverse functions in cell proliferation, morphogenesis, and meiosis. Curr. Biol. 12, 277–287.

Niwa, J., Ishigaki, S., Doyu, M., Suzuki, T., Tanaka, K., Sobue, G., 2001. A novel centrosomal ring-finger protein, dorfin, mediates ubiquitin ligase activity. Biochem. Biophys. Res. Commun. 281, 706–713.

Ozdamar, B., Bose, R., Barrios-Rodiles, M., Wang, H.R., Zhang, Y., Wrana, J.L., 2005. Regulation of the polarity protein Par6 by TGFbeta receptors controls epithelial cell plasticity. Science 307, 1603–1609.

Petroski, M.D., Deshaies, R.J., 2005. Function and regulation of cullin-RING ubiquitin ligases. Nat. Rev., Mol. Cell Biol. 6, 9–20.

Pickart, C.M., 2001. Mechanisms underlying ubiquitination. Annu. Rev. Biochem. 70, 503–533.

Pintard, L., Kurz, T., Glaser, S., Willis, J.H., Peter, M., Bowerman, B., 2003. Neddylation and deneddylation of CUL-3 is required to target MEI-1/Katanin for degradation at the meiosis-to-mitosis transition in *C. elegans*. Curr. Biol. 13, 911–921.

Portereiko, M.F., Mango, S.E., 2001. Early morphogenesis of the *Caenorhabditis elegans* pharynx. Dev. Biol. 233, 482–494.

Praitis, V., Casey, E., Collar, D., Austin, J., 2001. Creation of low-copy integrated transgenic lines in *Caenorhabditis elegans*. Genetics 157, 1217–1226.

Rappleye, C.A., Tagawa, A., Lyczak, R., Bowerman, B., Aroian, R.V., 2002. The anaphase-promoting complex and separin are required for embryonic anterior–posterior axis formation. Dev. Cell 2, 195–206.

Schnabel, H., Bauer, G., Schnabel, R., 1991. Suppressors of the organ-specific differentiation gene pha-1 of *Caenorhabditis elegans*. Genetics 129, 69–77.

Schnell, J.D., Hicke, L., 2003. Non-traditional functions of ubiquitin and ubiquitin-binding proteins. J. Biol. Chem. 278, 35857–35860.

Shakes, D.C., Sadler, P.L., Schumacher, J.M., Abdolrasulnia, M., Golden, A., 2003. Developmental defects observed in hypomorphic anaphase-promoting complex mutants are linked to cell cycle abnormalities. Development 130, 1605–1620.

Shimura, H., Hattori, N., Kubo, S., Mizuno, Y., Asakawa, S., Minoshima, S., Shimizu, N., Iwai, K., Chiba, T., Tanaka, K., Suzuki, T., 2000. Familial Parkinson disease gene product, parkin, is a ubiquitin-protein ligase. Nat. Genet. 25, 302–305.

Sijen, T., Fleenor, J., Simmer, F., Thijssen, K.L., Parrish, S., Timmons, L., Plasterk, R.H., Fire, A., 2001. On the role of RNA amplification in dsRNA-triggered gene silencing. Cell 107, 465–476.

Simmer, F., Tijsterman, M., Parrish, S., Koushika, S.P., Nonet, M.L., Fire, A., Ahringer, J., Plasterk, R.H., 2002. Loss of the putative RNA-directed RNA polymerase RRF-3 makes *C. elegans* hypersensitive to RNAi. Curr. Biol. 12, 1317–1319.

Sontheimer, E.J., 2005. Assembly and function of RNA silencing complexes. Nat. Rev., Mol. Cell Biol. 6, 127–138.

Timmons, L., Court, D.L., Fire, A., 2001. Ingestion of bacterially expressed dsRNAs can produce specific and potent genetic interference in *Caenorhabditis elegans*. Gene 263, 103–112.

van der Reijden, B.A., Erpelinck-Verschueren, C.A., Lowenberg, B., Jansen, J. H., 1999. TRIADs: a new class of proteins with a novel cysteine-rich signature. Protein Sci. 8, 1557–1561.

Wang, H.R., Zhang, Y., Ozdamar, B., Ogunjimi, A.A., Alexandrova, E., Thomsen, G.H., Wrana, J.L., 2003. Regulation of cell polarity and protrusion formation by targeting RhoA for degradation. Science 302, 1775–1779.

Yeong, F.M., 2004. Anaphase-promoting complex in *Caenorhabditis elegans*. Mol. Cell. Biol. 24, 2215–2225.

Yoon, C.H., Lee, J., Jongeward, G.D., Sternberg, P.W., 1995. Similarity of sli-1, a regulator of vulval development in *C. elegans*, to the mammalian proto-oncogene c-cbl. Science 269, 1102–1105.

Zamore, P.D., Tuschl, T., Sharp, P.A., Bartel, D.P., 2000. RNAi: double-stranded RNA directs the ATP-dependent cleavage of mRNA at 21 to 23 nucleotide intervals. Cell 101, 25–33.

Zhong, W., Feng, H., Santiago, F.E., Kipreos, E.T., 2003. CUL-4 ubiquitin ligase maintains genome stability by restraining DNA-replication licensing. Nature 423, 885–889.